



HAL
open science

Role of Electrostatic Interactions on Supramolecular Organization in Calf-Thymus DNA Solutions under Flow

L. Bravo-Anaya, Denis Roux, J. Soltero Martínez, Francisco Carvajal Ramos, Frédéric Pignon, Oonagh Mannix, Marguerite Rinaudo

► **To cite this version:**

L. Bravo-Anaya, Denis Roux, J. Soltero Martínez, Francisco Carvajal Ramos, Frédéric Pignon, et al.. Role of Electrostatic Interactions on Supramolecular Organization in Calf-Thymus DNA Solutions under Flow. *Polymers*, 2018, 10 (11), pp.1204. 10.3390/polym10111204 . hal-01989793

HAL Id: hal-01989793

<https://hal.science/hal-01989793>

Submitted on 25 Jan 2019

HAL is a multi-disciplinary open access archive for the deposit and dissemination of scientific research documents, whether they are published or not. The documents may come from teaching and research institutions in France or abroad, or from public or private research centers.

L'archive ouverte pluridisciplinaire **HAL**, est destinée au dépôt et à la diffusion de documents scientifiques de niveau recherche, publiés ou non, émanant des établissements d'enseignement et de recherche français ou étrangers, des laboratoires publics ou privés.



Distributed under a Creative Commons Attribution 4.0 International License

1 Type of the Paper (Article, Review, Communication, etc.)

2 Role of Electrostatic Interactions on Supramolecular 3 Organization in Calf-Thymus DNA Solutions under 4 Flow

5 L. Mónica Bravo-Anaya ^{1,2}, Denis C. D. Roux ^{1,*}, J. Félix Armando Soltero Martínez ²,
6 Francisco Carvajal Ramos ³, Frédéric Pignon ¹, Oonagh Mannix ⁴ and Marguerite Rinaudo ^{5,*}

7 ¹ University Grenoble Alpes, CNRS, Grenoble INP, LRP, F-38000 Grenoble (France);
8 monik_ayanami@hotmail.com, Denis.Roux@univ-grenoble-alpes.fr, frederic.pignon@univ-grenoble-
9 alpes.fr

10 ² Universidad de Guadalajara, Departamento de Ingeniería Química. Blvd. M. García Barragán #1451, C.P.
11 44430, Guadalajara, Jalisco (México); jfasm@hotmail.com

12 ³ Universidad de Guadalajara, CUTonalá, Departamento de Ingenierías, Nuevo Periférico #555 Ejido San
13 José Tatepozco, C.P. 45425, Tonalá, Jalisco (México); iq_fcr@yahoo.com.mx

14 ⁴ European Synchrotron Radiation Facility, 38000 Grenoble (France); oonmannix@gmail.com

15 ⁵ Biomaterials applications, 6 rue Lesdiguières, 38000 Grenoble (France); marguerite.rinaudo@sfr.fr

16 * Correspondence: marguerite.rinaudo38@gmail.com; Tel.: +33-611-434-806
17 denis.roux@univ-grenoble-alpes.fr; Tel.:+33-699-296-709

18 **Abstract:** Previous investigations were conducted on two concentrations of DNA solution: 4
19 mg/mL, for which it has been shown that no supramolecular organization is induced under flow at
20 low shear rates; and 10 mg/mL, in which a liquid crystalline-type texture is formed under flow at
21 low shear rates, attesting to an orientation of pre-organized chains. Rheological experiments are
22 discussed and their results supported by small-angle X-ray scattering (SAXS) and flow birefringence
23 visualization experiments. Scattering from polyelectrolytes has a characteristic signal, which is here
24 observed in SAXS, showing a strong correlation peak between charged chains in water, for both
25 concentrations. This peak is weaker in the presence of 0.01 M NaCl and suppressed in salt excess at
26 0.1 M NaCl. No plateau in the $\sigma(\dot{\gamma})$ plot was observed in analysis of rheological experiments on low
27 DNA concentration (4 mg/mL). As typically observed in polyelectrolyte systems both the dynamic
28 moduli and shear viscosity were higher in water as electrostatic forces dominate, than in the
29 presence of salt, especially at low shear rates. The rheological results for concentrations of 0.01 M
30 NaCl are lower than in water as expected due to partial screening of electrostatic repulsions.
31 Rheological data for concentrations of 0.1 M NaCl are unexpected. Electrostatic forces are partially
32 screened in the low salt concentration, leading to a drop in the rheological values. For high salt
33 concentration there are no longer interchain repulsions and so steric interactions dominate within
34 the entangled network leading to the subsequent increase in rheological parameters. Regardless of
35 the solvent, at high shear rates the solutions are birefringent. In the 10 mg/mL case, under flow,
36 textures are formed at relatively low shear rate before all the chains align going to a pseudo-nematic
37 liquid crystalline phase at high shear rate. The electrostatic repulsion between semi-rigid chains
38 induces a correlation between the chains leading to an electrostatic pseudo-gel in water and loosely
39 in 0.01M NaCl at low stress applied. To our knowledge, this is the first time that such behavior is
40 observed. In 0.1M NaCl, DNA behavior resembles the corresponding neutral polymer as expected
41 for polyelectrolyte in salt excess, exhibiting a yield stress. When texture appears in water and in
42 0.01M NaCl, a critical transition is observed in rheological curves, where the viscosity decreases
43 sharply at a given critical shear stress corresponding to a plateau in the $\sigma(\dot{\gamma})$ plot also observed in
44 creep transient experiment.

45 **Keywords:** DNA; external ionic concentration; rheology; birefringence; SAXS; electrostatic
46 interactions
47

48 1. Introduction

49 DNA is a semi-rigid polyelectrolyte with a high persistence length ($L_p \sim 50$ nm) [1-3].
50 Understanding electrostatic interactions between stiff chain segments in DNA, and polyelectrolyte
51 solutions is important, both fundamentally and for biological applications [4]. These interactions
52 depend on the charge density of the polyelectrolyte favoring parallel alignment of the chains, and on
53 the external salt concentration screening the electrostatic repulsions [5]. Due to condensed
54 counterions in 1-1 electrolyte, there exists a range of distances less than the Debye length where
55 polyions attract each other [6-10]. Birefringence has previously shown that textures corresponding to
56 orientated, ordered domains are induced under shear flow for DNA concentrations higher than 5
57 mg/mL at low ionic concentration [11]. A schematic representation of the evolution of these solutions
58 at rest and under flow was proposed [11]. To complete our previous work, the rheological behavior
59 of DNA in aqueous solution is studied: at two polymer concentrations (4 mg/mL and 10 mg/mL); in
60 water, and in the presence of two ionic concentrations: 0.01M and 0.1M NaCl; to investigate the
61 influence of ionic concentration on rheological behavior and on birefringence induced under flow.
62 The polymer concentrations are chosen such that DNA is in the semi-dilute regime with a low degree
63 of entanglement. SAXS experiments complete the data studying in the same solvent conditions, long-
64 range interactions between chains.
65

66 2. Materials and Methods

67 2.1. Materials and solutions preparation

68 High-molecular weight calf-thymus DNA (MW=6 560 000 g/mol) was used to prepare solutions
69 at concentrations of 4 and 10 mg/mL [11]. Ultrapure water and NaCl anhydrous were used to obtain
70 different external ionic concentrations: 0, 0.01 and 0.1 M NaCl. The double helix conformation of
71 DNA is stabilized under these conditions. Vials were closed and sealed with Parafilm® to prevent
72 water evaporation and concentration changes. Solutions were stored at 4 °C to prevent degradation.
73 Sigma-Aldrich Company supplied all reagents.
74

75 2.2. Rheometric measurements.

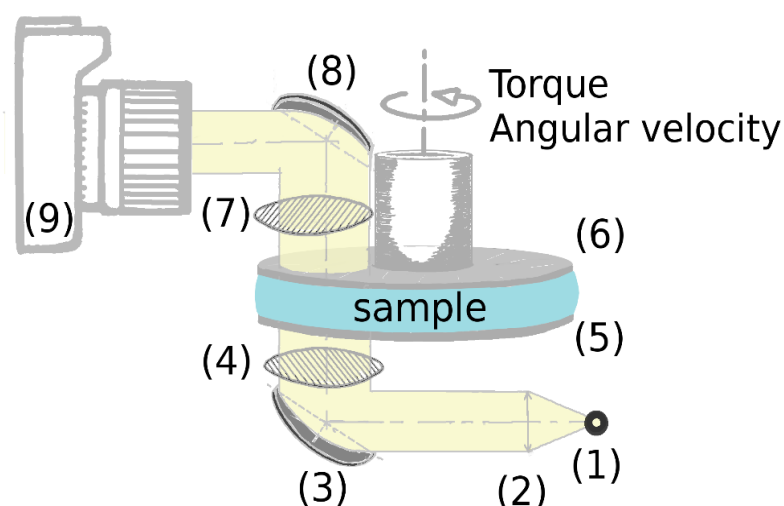
76 DNA rheology was studied at 25 °C using a DHR-3 rheometer from TA Instruments Company
77 and a MCR-501 rheometer from Anton-Paar Company. Two geometries were used: a steel cone-plate
78 geometry with 40 mm diameter and an angle of 0.035 rad was used in DHR3 rheometer; and a glass
79 plate-plate geometry with a 50 mm diameter was employed with the MCR501 rheometer to observe
80 birefringence under crossed polarizers. Birefringence visualizations are integrated through the gap
81 with a wave vector in the direction of the velocity gradient. A solvent cap was used to prevent solvent
82 evaporation.

83 To define the linear viscoelastic regime oscillatory strain sweeps were undertaken at an angular
84 frequency of 10 rad/s in the strain range from 0.01 to 100 %. Frequency sweeps were performed at 1%
85 strain within the linear viscoelastic regime of G' and G'' in a frequency range ω from 0.01 to 100 rad/s,
86 with at least 5 points per decade. Simple steady state shear was measured at shear rates from 10^{-3} to
87 $1\ 000\ s^{-1}$ with at least 5 points per decade. Due to thixotropic behavior of 10mg/mL DNA solution, in
88 order to reduce the time to obtain the steady state, increasing/decreasing ramps were imposed.
89 Firstly, a rapid shear rate increase from 0 to $100\ s^{-1}$ was applied in 160 s followed directly by a
90 decreasing ramp in 3000 s.

91 Transitory experiments in creep flow consist of applying constant stresses from 10^{-2} to 20 Pa and
92 observing the creep flow over a time up to 10^3 s for each applied stress. In the first part of the shear
93 rate (time response), the transient regime is characterized by damped oscillations due to a coupling
94 between tool inertia and solution viscoelasticity. Final constant shear rate corresponds to the steady
95 state.

96 2.3. Flow birefringence visualizations

97 Birefringence was tested using a glass plate-plate configuration with an adapted gap, of at least
 98 0.2 mm, such that the geometry was filled completely with DNA solution. This geometry is placed
 99 between crossed polarizers, one below and another just above the sample (**Figure 1**). The sample was
 100 illuminated vertically by a white source of light reflected by a mirror placed at 45° below the first
 101 polarizer under the geometry. A second mirror, placed at 45° above the upper polarizer, collected
 102 pictures at different imposed shear rates with CMOS device cameras (Canon 100 D or Sony DSLR-
 103 A580) and adapted commercial zooms.



104

105 **Figure 1.** Schematic description of the home-made birefringence set-up on the rheometer MCR-501.
 106 (1) white source, (2) lens, (3) and (8) mirrors, (4) and (7) crossed polarizers, (5) and (6) plate-plate
 107 geometry and (9) camera.

108 2.4. Small-angle X-ray scattering (SAXS) measurements

109 The SAXS experiments were performed on ID02 high brilliance beamline at European
 110 Synchrotron Radiation Facility (ESRF, Grenoble, France). DNA solutions were analyzed under
 111 controlled temperature (25 ± 1 °C) in a flow-through capillary cell (diameter ~ 2 mm). An incident
 112 monochromatized X-ray beam at wavelength of 0.995 \AA was used. Scattered intensities were recorded
 113 on a two-dimensional CCD detector at sample-to-detector distances of 0.75 m and 8 m. The scattering
 114 intensity distribution as a function of scattering vector was obtained by radial integration of 2D
 115 scattering pattern. Background subtraction was done using a cell filled with water for all samples.
 116 This is not a perfect background for solutions with high salt concentration, as seen in the increased
 117 intensity in the high- q region. As scattering from the salt ions makes no contribution in the low- q
 118 region this does not change outcome of the analysis.

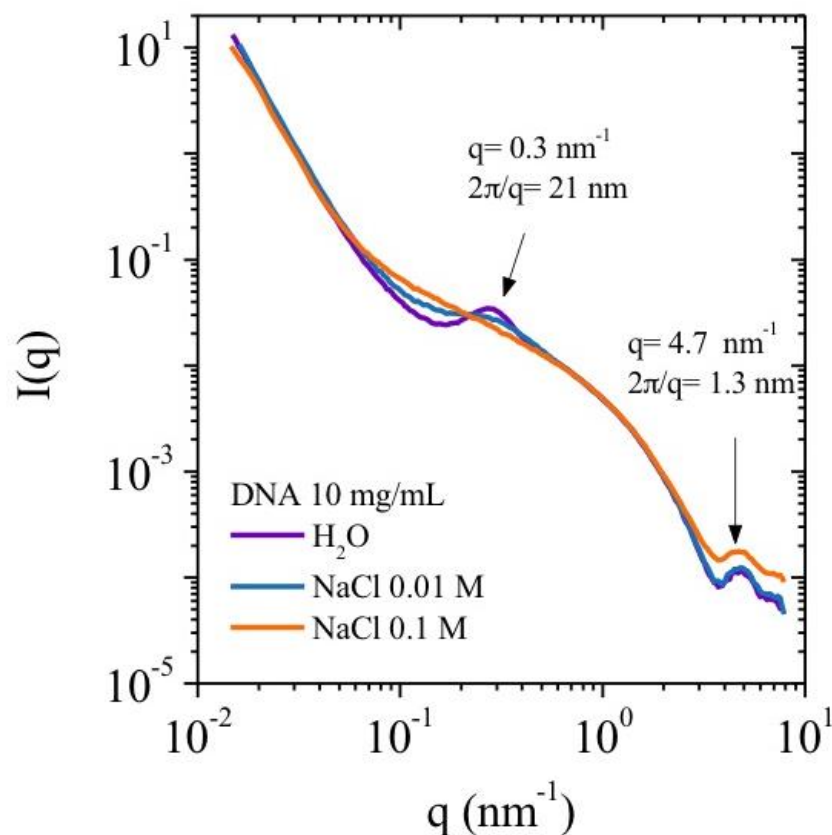
119 3. Results and discussion

120 3.1. X-Ray scattering

121 Both X-ray scattering and rheological experiments were performed in identical experimental
 122 conditions. The influence of ionic concentration is examined by adding external salt. A correlation
 123 peak is observed in the SAXS data, this is evidence of long-range electrostatic repulsions. These
 124 repulsions are caused by interactions between polymer chains forming a local network with a
 125 preferential inter-chain distance.

126 The correlation peak for polyelectrolyte solution in absence of external salt is located at q^* such
 127 as $2\pi/q^* = 21 \text{ nm}$ at 10 mg/mL DNA solution in water. It is progressively depressed in the presence of
 128 external salt as shown for 0.01 M NaCl and is suppressed in 0.1 M NaCl . Correlation peak extinction

129 in salt excess is typically observed in polyelectrolyte solutions and also observed in neutron and light
 130 scattering experiments [12-15]. At high q values ($q > 3 \text{ nm}^{-1}$), the form factor of DNA is independent
 131 of the salt content (**Figure 2**) and agrees with the model given by Pringle and Schmidt [16].



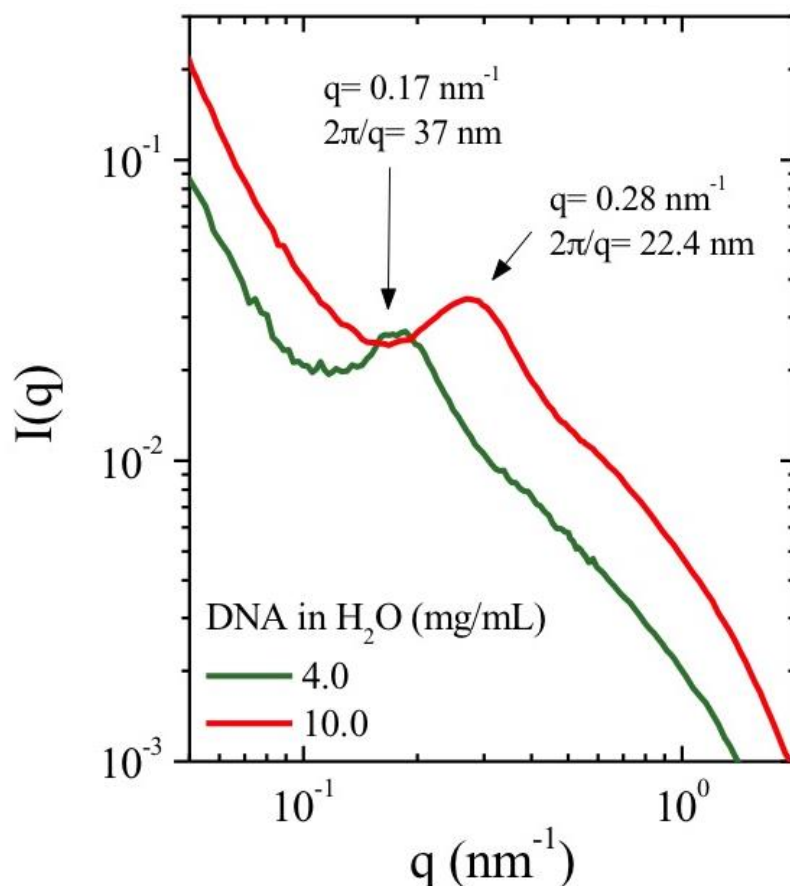
132

133 **Figure 2.** SAXS intensity $I(q)$ as a function of the wave vector q at different external salt concentrations.

134 DNA solution at 10 mg/mL at 25°C.

135 The influence of polyelectrolyte concentration is shown in **Figure 3**. The SAXS intensity profile
 136 is presented in the absence of external salt at 4 and 10 mg/mL. q^* , corresponding to the maximum in
 137 the SAXS intensity as a function of q , decreases when the polymer concentration (C_p) decreases as
 138 found in the literature. The values of q^* vary following a scaling law $q^* \sim C_p^{1/2}$ in agreement with a
 139 hexagonal packing with a correlation distance between packed strands, indicating a preferential
 140 distance between chains. At 4 mg/mL, $q^* = 0.17 \text{ nm}^{-1}$ which gives a predicted value of $q^* = 0.27 \text{ nm}^{-1}$ at
 141 10 mg/mL using this scaling law. This value is in agreement with the experimentally determined
 142 value of $q^* = 0.28 \text{ nm}^{-1}$.

143 These results confirm our hypothesis on the formation of organized chains.¹¹ The SAXS values
 144 obtained indicate a nearly homogeneous distribution of stiff interacting chains throughout the
 145 solution. This agrees with the schematic representation given by Odijk for the case where polymer
 146 persistence length is greater than the distance between two chains [4].



147

148 **Figure 3.** SAXS intensity $I(q)$ as a function of the wave vector q for 4mg/mL and 10 mg/mL DNA
 149 concentrations at 25 °C.

150 To reflect the role of inter-chain electrostatic repulsion the DNA Debye-lengths were estimated.
 151 This includes the DNA counterion contribution (C_p (ion/L) = $[(0.12/370)*C$ (g/L)] where 0.12 is the
 152 activity coefficient of counterions and 370 the average molar mass of the nucleic repeat unit; and the
 153 ionic contribution of external salt (**Table 1**). In 0.1M NaCl the behavior should approach the
 154 corresponding neutral polymer. In these experimental conditions, the influence of the ionic
 155 concentration, as demonstrated by the estimated Debye length, is low compared to the intrinsic value
 156 of the persistence length, around 50 nm.

157 **Table 1.** Estimation of the Debye screening length κ^{-1} expressed in nm.

Polymer concentration (mg/mL)	κ^{-1} water (nm)	κ^{-1} 0.01M NaCl (nm)	κ^{-1} 0.1M NaCl (nm)
4	8.42	2.83	0.94
10	5.36	2.61	0.93

158 Finally, it is important to mention the large increase of $I(q)$ at low q values indicating the
 159 formation of supramolecular structure as proposed in our model [11]. Moreover, the intensity profile
 160 at low q values ($q \sim 10^{-2} \text{ nm}^{-1}$) agrees with the existence of aggregates with constant dimension for H₂O
 161 and 0.01M NaCl [17]. In salt excess condition, $I(q)$ slope is lower indicating a significant change of
 162 structure (**Figure 2**). Unfortunately, this does not allow direct determination of the persistence length
 163 from experimental data as obtained previously on another polyelectrolyte [18].

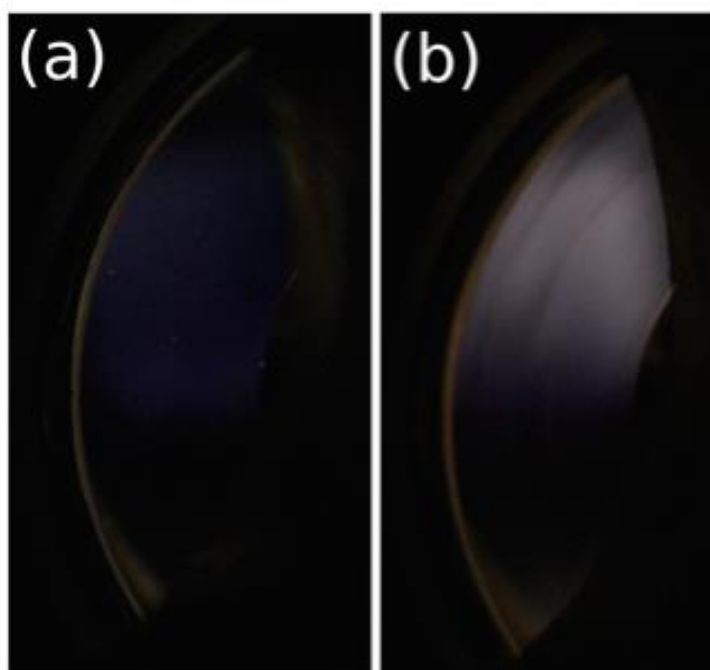
164 **3.2. Birefringence and texture under shear**

165 Data previously obtained for DNA solution at 10 mg/mL, in TE buffer at ionic concentration
 166 around 0.01M, were completed with birefringence observations, as a function of shear rate. The two
 167 polymer concentrations are chosen as at 4 mg/mL the absence of birefringent texture was previously
 168 demonstrated, while texture was observed at 10 mg/mL. This enables investigation of influence of
 169 texture on rheological behavior.

170 In **Table 2** it is shown that salt has a critical role in observing birefringence, and birefringent
 171 textures. **Figures 4** and **5** present examples of birefringence and the textures observed.

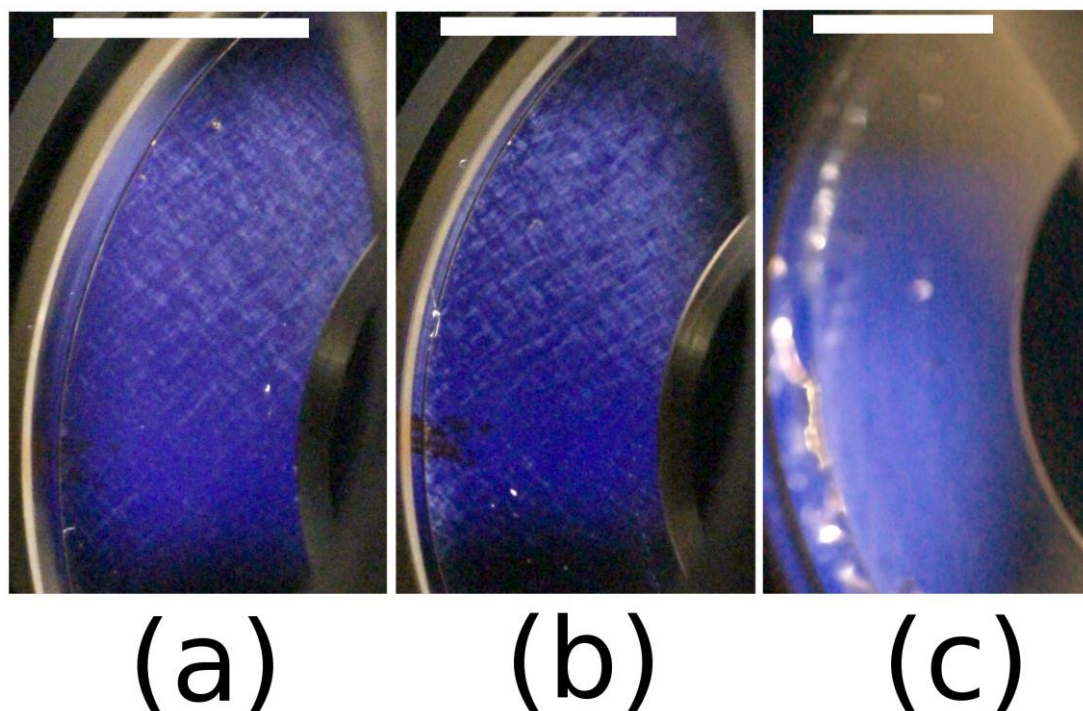
172 **Table 2.** Influence of polymer and ionic concentration on the critical shear rate for birefringence and
 173 texture formation.

Solvent properties	H ₂ O	0.01M NaCl	0.1M NaCl
4 mg/mL Birefringence	$\sigma = 5$ Pa	$\sigma = 4.6$ Pa	$\sigma = 4.5$ Pa
4 mg/mL Texture	NO	NO	NO
10 mg/mL Birefringence	$\dot{\gamma} > 1$ s ⁻¹ $\sigma = 8$ Pa	$\dot{\gamma} > 1$ s ⁻¹ $\sigma = 9$ Pa	$\dot{\gamma} \sim 100$ s ⁻¹ $\sigma = 10$ Pa
10 mg/mL Texture	$\dot{\gamma} \sim 1-10$ s ⁻¹ $\sigma = 10$ Pa	$\dot{\gamma} \sim 10$ s ⁻¹ $\sigma = 15$ Pa	Heterogeneous birefringent domains $\sigma = 8$ Pa



174

175 **Figure 4.** Birefringence of DNA solution at 4 mg/mL in 0.1M NaCl under shear a) at 10⁻³ s⁻¹ b) at 500
 176 s⁻¹.



177

178
179
180
181

Figure 5. Supramolecular organization of 10 mg/mL DNA solution sheared at 25°C: a) Texture obtained in water; b) in 0.01M NaCl; c) heterogeneous birefringence in 0.1M NaCl. The white bars represent the scale of 10 mm. Two videos for solutions in water and in 0.1M NaCl under shear are joined in SI.

182
183
184
185
186
187
188

These data show no texture is formed at concentrations of 4mg/mL, confirming our previous observations [11], however birefringence is observed at relatively high shear stress (around 4.5 Pa). Our model of DNA consists of the presence of ordered domains, as evidenced by the correlation peak in SAXS data. These domains are loosely connected by extended single chains. At high shear stress the domains are fully orientated, forming a pseudo-nematic phase. In a previous study, the orientation of semi-rigid chains was directly demonstrated by neutron scattering on xanthan (a semi-rigid polysaccharide) solution under shear 15.

189
190
191
192
193
194
195
196

The role of polymer concentration on the supramolecular organization of DNA in solution is demonstrated for the 10 mg/mL DNA concentration. Birefringence occurs at low shear rates, but larger shear stress due to the high solution viscosity. At 10mg/mL, liquid crystalline like textures occur over shear rates of 1s^{-1} confirming our previously published data [11]. In the presence of salt at 0.1M NaCl, heterogeneous birefringent elongated domains appear under shear. The density of these domains progressively increases to form an almost homogeneous nematic phase. In all these experiments, a slightly negative normal force is observed when chains are orientated. It increases when the textures appear and become slightly positive.

197

3.3. Rheological behavior

198
199
200
201
202
203
204
205

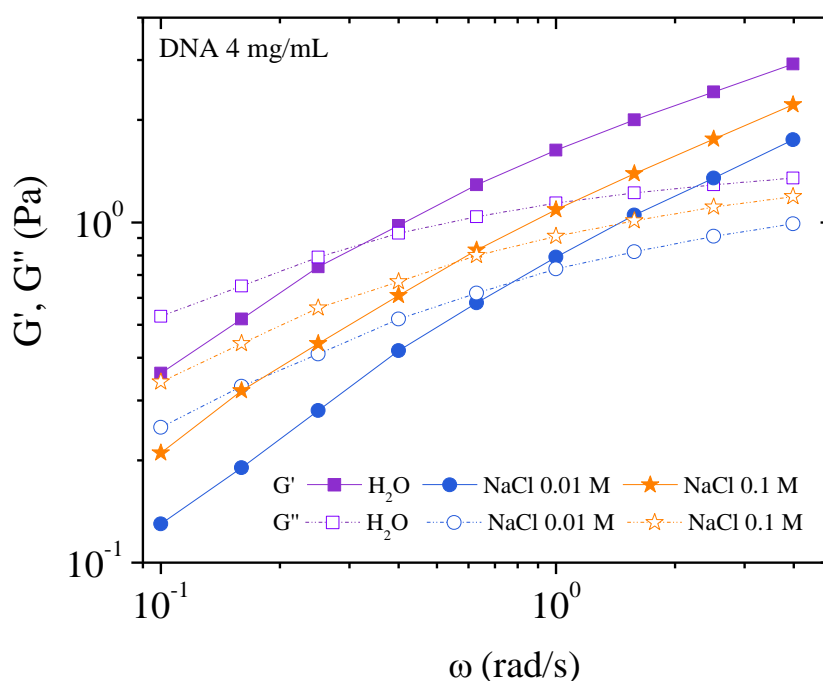
To complete our previous rheological experiments on DNA solutions [11], we examined the rheological behavior at different external salt contents: in the absence of salt, and at 0.01M and 0.1M NaCl. Electrostatic repulsions are maximum in the absence of salt and progressively screened with the addition of salt. At 0.1 M in which the Debye length is small (**Table 1**), the behavior goes to that of the corresponding neutral polymer involving steric hindrance between semi-rigid chains. The influence of external salt, on viscometric measurements, is well described in literature [5]. Two different polymer concentrations are tested to evidence clearly the influence of texture on the rheological behavior in the semi-dilute regime, 4 mg/mL being the model for absence of texture.

206 3.3.1. Behavior at 4 mg/mL

207 This solution is considered as a model for an entangled semi-dilute system in which the role of
 208 salt concentration, intrinsic stiffness, and absence of “liquid crystalline” ordered domains or texture
 209 are investigated as a function of the ionic concentration.¹¹

210 3.3.1.1. Dynamic measurements

211 Rheological experiments were performed in the linear domain. The influence of external salt
 212 concentration (C_s) is shown in Figure 6 and summarized in **Table 3**. It is seen that the bulk relaxation
 213 time is longer in water, as is the stiffness of the system, due to stronger inter-chain repulsion requiring
 214 a stronger stress to perturb the supramolecular structure composed of correlated chains.



215

216 **Figure 6.** Elastic (G') and viscous (G'') moduli as a function of the angular frequency at 25°C for
 217 different solvent ionic concentrations 0, 0.01M and 0.1M NaCl for ADN 4 mg/mL.

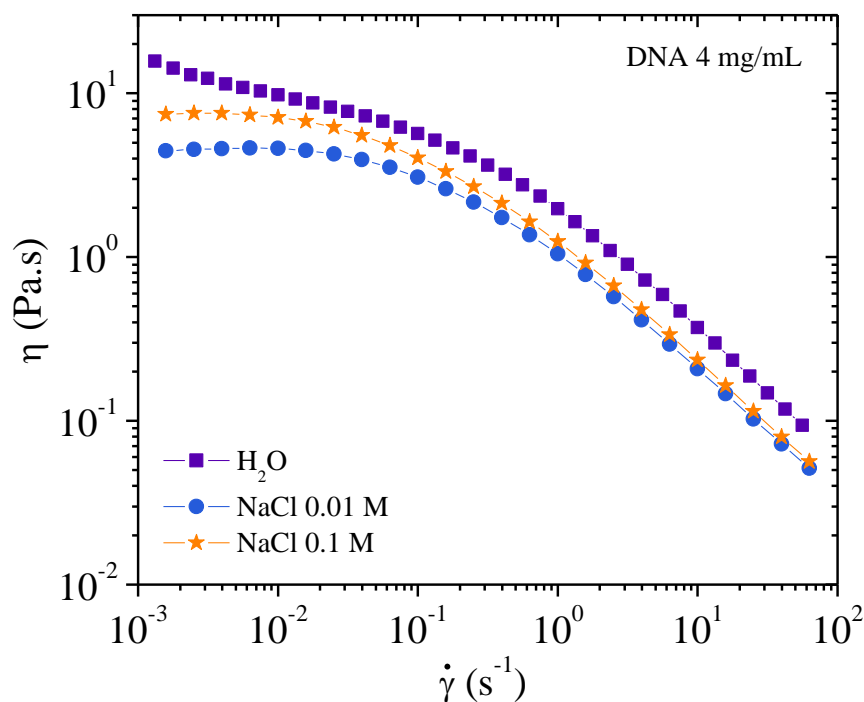
218 The G' - G'' crossing transition ω_0 does not increase linearly with salt concentration. Firstly, ω_0
 219 increases upon addition of salt (0.01M NaCl). This demonstrates a decrease in electrostatic forces,
 220 further evidenced by the reduction of the correlation peak in SAXS. Then ω_0 decreases upon further
 221 addition of salt (0.1M NaCl). This state resembles that of the corresponding uncharged polymer with
 222 stronger entangled contacts than in the case of simple electrostatic repulsion (seen for the 0.01 M NaCl
 223 concentration) leading to an increase in G' .

224 **Table 3.** Characterization of the elastic (G') and loss (G'') moduli at the transition for different ionic
 225 concentrations.

	H ₂ O	0.01M NaCl	0.1M NaCl
G_0 (Pa)	0.84	0.68	0.78
ω_0 (rad/s)	0.31	0.82	0.59
η_0 (Pa.s) for $\dot{\gamma} \rightarrow 0 \text{ s}^{-1}$	18 at $\dot{\gamma} = 10^{-3} \text{ s}^{-1}$	4.1	7.2

226 3.3.1.2. Flow measurements

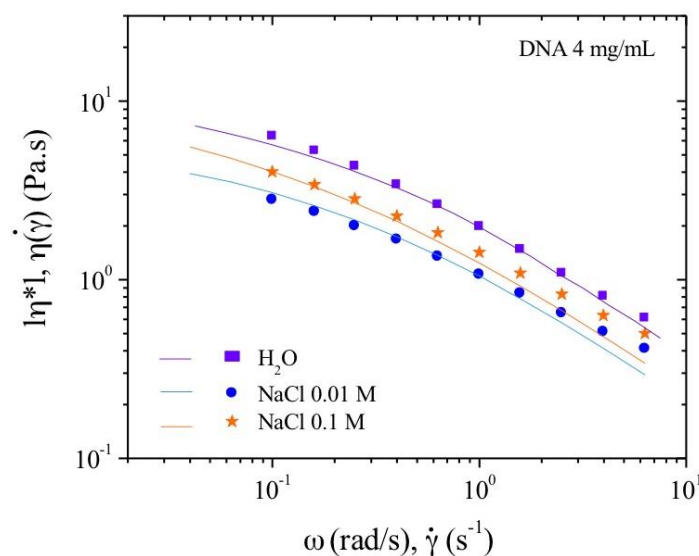
227 Viscosities as a function of the shear rate are plotted in Figure 7. The well-known behavior of
 228 polyelectrolyte viscosity is observed in water. In absence of external electrolyte, the viscosity
 229 increases rapidly when the shear rate decreases due to strong electroviscous effects [20]. In 0.01M
 230 NaCl, the screening gives a pseudo plateau at low shear rate when the ionic contribution of DNA is
 231 in the same range as the solvent ionic concentration as discussed previously [5].



232

233 **Figure 7.** Flow viscosities of 4 mg/mL DNA solutions as a function of the shear rate at 25°C solvents
 234 with different ionic concentrations: 0, 0.01M and 0.1M NaCl.

235 In excess of salt at 0.1M NaCl, the DNA solution behaves as the corresponding neutral polymer
 236 with a viscous plateau below 0.02 s⁻¹. The viscosity is lower than DNA solution in water but larger
 237 than in 0.01M NaCl due to screening of electrostatic long-range interactions. This is directly related
 238 to the dynamic behavior discussed previously (**Figure 6**). Over $\dot{\gamma} > 1 \text{ s}^{-1}$, the viscosities are nearly the
 239 same in both NaCl-containing solvents corresponding to progressive flow alignment. Birefringence
 240 measurements shows a progressive increase interpreted as an alignment of domains culminating in
 241 the alignment of all chains forming a pseudo-nematic phase (see pictures in **Figure 4**). To demonstrate
 242 the validity of the dynamic and shear viscosities, the Cox Merz representation is given in **Figure 7**.



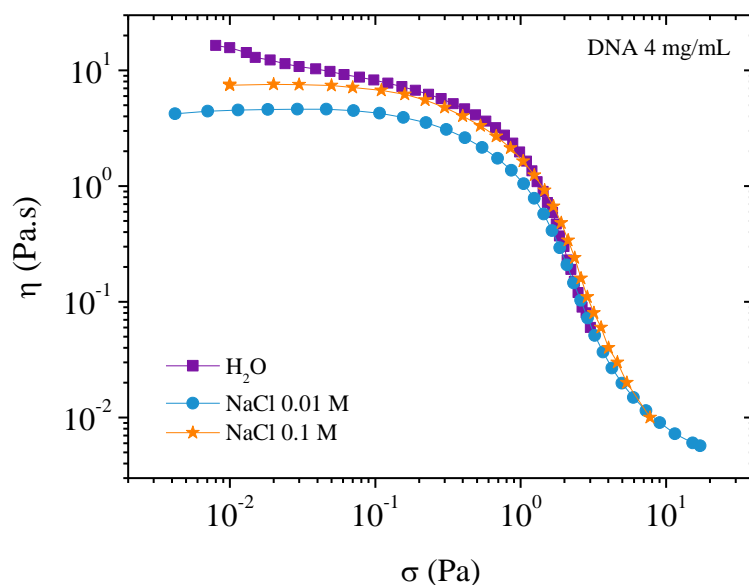
243

244 **Figure 8.** Cox Merz overlay for 4mg/mL DNA solution at 25°C in different ionic concentrations: 0,
 245 0.01M and 0.1M NaCl. Continuous lines represent the flow viscosities and the dots represent dynamic
 246 oscillatory viscosity measurements.

247 **Figure 8** shows the complex viscosity derived from dynamic experiments and viscosity from
 248 flow behavior are in agreement, for the frequency range covered here, corresponding to the Cox Merz
 249 rule. In the presence of external salt, there is dissociation of the two types of viscosity curve over 1
 250 s⁻¹, with flow viscosities being lower than the complex viscosities. This is related to the screening of
 251 electrostatic repulsions and subsequent increase in the elastic contribution of the chains.

252 Observing a decrease in viscosity in polyelectrolyte solutions is a normal behavior upon
 253 increasing salt concentration due to a decrease in the electroviscous effects. However, upon complete
 254 electrostatic screening, as in the case of 0.1 M NaCl, the viscosity increases at low shear rate compared
 255 with DNA solution in 0.01M NaCl. This is due to the large steric interactions present in the semi-
 256 dilute entangled solution.

257 In **Figure 9**, the viscosity is plotted as a function of the applied shear stress. At low shear stresses
 258 viscosity of the 0.1M NaCl solution is lower than that of water but higher than the 0.01M NaCl
 259 solution. A plateau is observed when NaCl is present but not in water alone. In water the viscosity
 260 increases rapidly at very low shear stress this is related to the existence of a yield stress caused by an
 261 electrostatic network formation. This point will be discussed later for higher polymer concentration.



262

263

264

Figure 9. Viscosity as a function of the applied shear stress on 4mg/mL DNA solutions in different solvents: 0, 0.01M and 0.1M NaCl at T=25°C.

265

266

267

268

269

270

Progressively increasing the stress induces orientation of the chains regardless of the ionic concentration. This leads to the curves superimposing for stresses around 2 Pa (over 1 s⁻¹) corresponding to the appearance of birefringence, and for stress greater than 4 Pa complete orientation of chains and a pseudo-nematic phase is observed. Figure 9 shows a smooth transition in $\eta(\dot{\gamma})$ curve confirming the absence of a plateau on $\sigma(\dot{\gamma})$ representation as shown in our previous work.

271

3.3.2. Behavior at 10 mg/mL

272

273

274

Under the same conditions as for DNA 4mg/mL solution, dynamic experiments were performed in the linear domain. The important difference concerns the lower stress at which birefringence appears, and the presence of texture in water and low ionic concentration (**Table 2, Figure 5**).

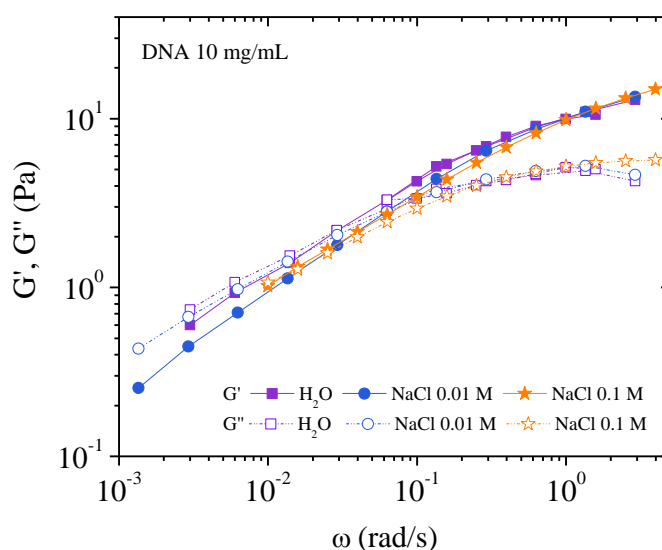
275

3.3.2.1. Dynamic measurements

276

277

At low frequencies the behavior, as observed by dynamic rheological measurements, is nearly identical in the three solvents. An original behavior is observed in **Figure 10**.



278

279

280

Figure 10. Elastic and viscous moduli obtained by dynamic oscillatory rheology for 10 mg/mL DNA solution at different ionic concentrations: 0, 0.01M and 0.1M NaCl ($T=25^{\circ}\text{C}$).

281

282

283

284

285

286

287

288

289

290

291

292

G' and G'' are superimposed in water and additionally, $G'=G''$ up to $\omega\sim 0.08$ rad/s. Below $\omega\sim 0.08$ rad/s, $G'(\omega)=G''(\omega)=G^{0.5}$ the exponent equals 0.5, in agreement with the criterion of Winter et al. [21-23]. The criterion of Winter et al. states that a network can form, for low frequencies, in the semi-dilute entangled DNA solution. This network is caused by strong electrostatic repulsion impeding the movement of single chains until some critical stress is applied. In 0.01M and 0.1M NaCl, a slight decrease of G' is observed indicating the decrease of the electrostatic repulsion. At higher frequency, $G'>G''$ is related to the modification of the supramolecular structure of the fluids corresponding to transition from solid like behavior to a liquid flowing phase which occurs above the critical gel condition ($\omega=0.08$ rad/s). Above 0.1 rad/s, the moduli overlap in water and NaCl solutions as described by Winter and Mours for a critical gel (Figure 12 of ref. 22). In the range of high frequencies, G'' is nearly constant without influence of salt content being not affected by the degree of crosslinking indicating the behavior of a classical viscoelastic fluid.

293

3.3.2.2. Flow measurements

294

295

296

297

298

299

300

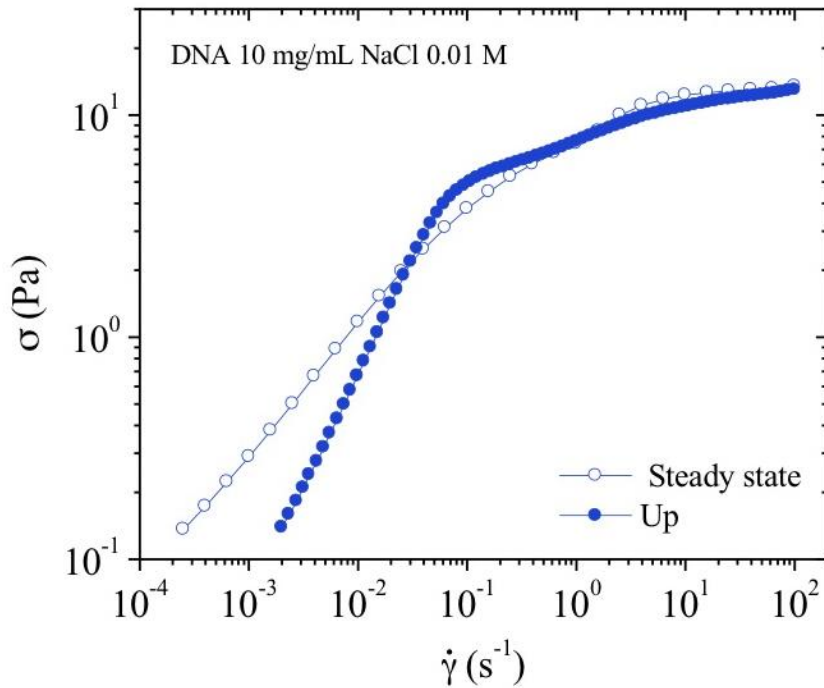
301

302

303

304

It is difficult to reproduce viscosity measurements at low shear rate for concentrated systems [24-28]. This is illustrated, in **Figure 11** in 0.01M NaCl. Firstly, an increasing shear rate is imposed resulting in a stress versus shear rate dependence with a slope of 1 up to around 0.1 s^{-1} , corresponding to an apparent Newtonian plateau. Above 0.1 s^{-1} , shear stress follows a smooth evolution up to 100 s^{-1} corresponding to a bulk flow regime. On the decreasing shear rate ramp, the shear stress decreases taking values larger than those obtained during the increasing ramp at low shear rate. The increase behavior is characteristic of slipping at the walls and thixotropy occurring in more concentrated solutions [24,29]. In concentrated system, those generic flow curves are the signature of an apparent yield stress fluid with slipping as confirmed hereinafter. In fact, the yield stress is proportional to the elastic shear modulus [24], which is nearly the same in the three solvents with a small influence of electrostatic interactions due to the presence of external salt (**Figure 10**).



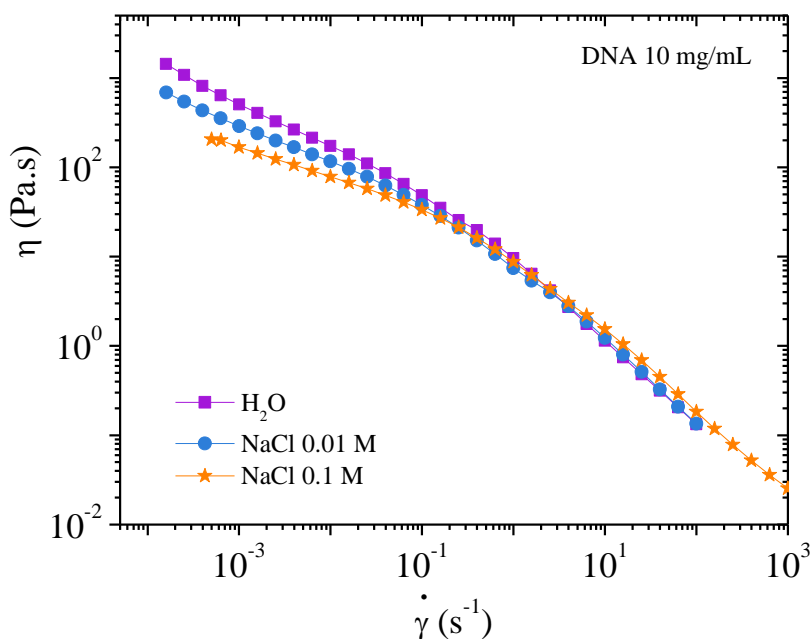
305

306
307

Figure 11. Shear stress as a function of the shear rate obtained for an increasing followed by a decreasing shear rate ramp on DNA solution in 0.01M NaCl at T=25°C.

308
309
310
311
312
313

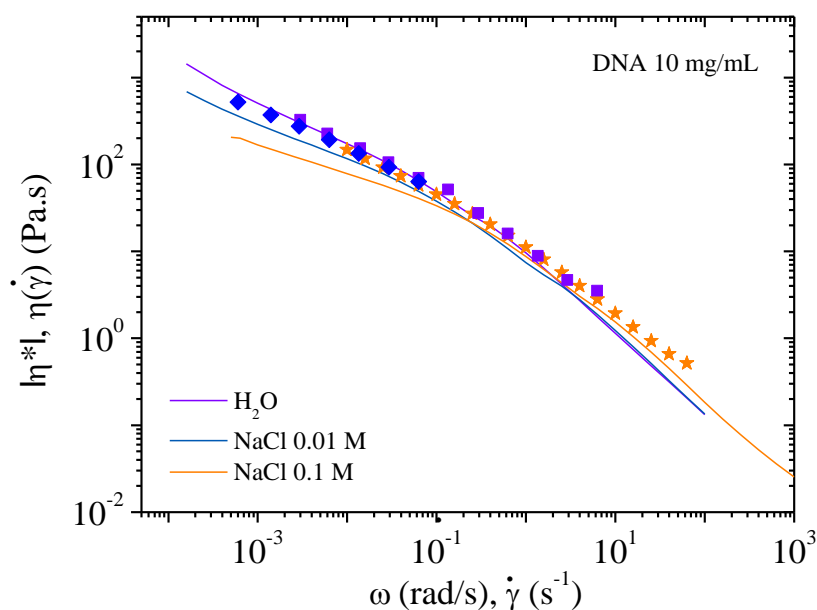
Figure 12 is a plot of viscosity against shear rate. The points were obtained while decreasing the shear rate. It can be seen that the values are lower for solutions with added salt. This is expected behavior for polyelectrolytes. In all three cases, viscosity increases at low shear rate in agreement with the existence of a yield stress. Over 10^{-1} s^{-1} the viscosities in the three solvents are overlapping in agreement with the behavior in dynamic rheological measurements. The flow viscosity and complex viscosity from the oscillatory behavior are shown in **Figure 13**.



314

315
316

Figure 12. Flow viscosities as a function of the shear rate for DNA 10 mg/mL solutions in the 3 solvents: H₂O, 0.01M and 0.1M NaCl. Values are taken on the decreasing shear rate ramp.

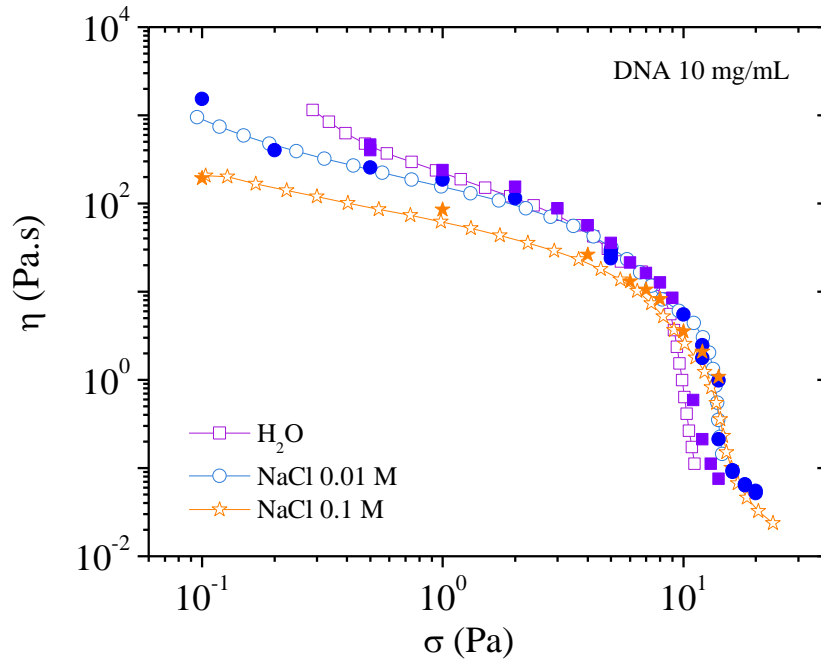


317

318 **Figure 13.** Cox Merz overlay for 10 mg/mL DNA solution at 25°C in different ionic concentrations: 0,
 319 0.01M and 0.1M NaCl. Continuous lines represent the flow viscosities and the dots represent dynamic
 320 oscillatory viscosities measurements.

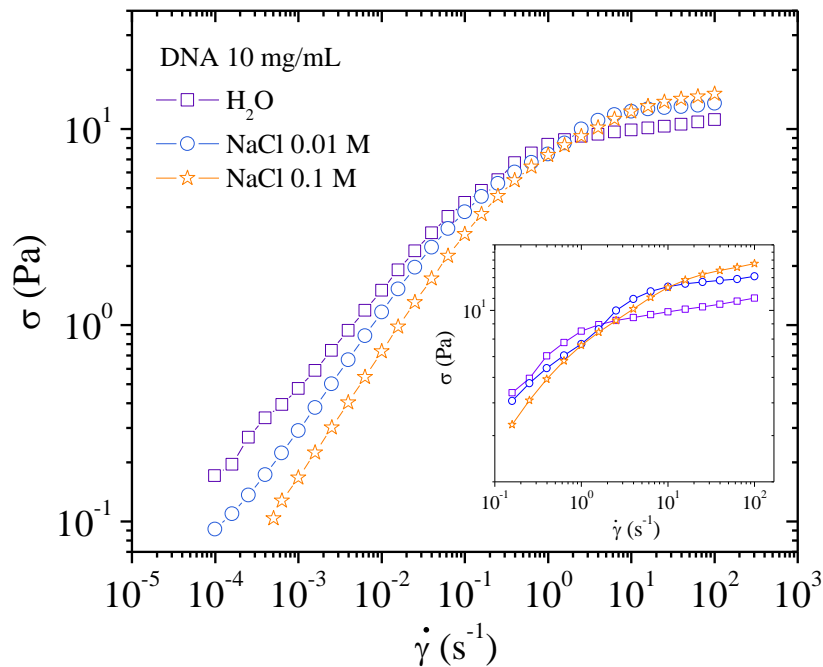
321 From these data, the complex viscosity fairly agrees with the shear viscosity measurements
 322 following the Cox Merz rule (**Figures 10 and 12**) for which G' and G'' overlap over $\omega=10^{-1}$ rad/s. At
 323 low frequency, in the range of gel-like behavior, the Cox Merz rule is no more valid in presence of
 324 external salt probably due to slip at the wall in absence of any supramolecular structural change as
 325 indicated in **Table 2**.

326 To relate the rheological behavior with supramolecular organization, viscosity is plotted as a
 327 function of the applied stress in **Figure 14**. It is shown that the stress needed to orientate the
 328 electrostatic network with flow direction in water is around 10 Pa much larger than for 4 mg/mL
 329 DNA solution (around 2 Pa, **Figure 9**). In these curves, two series of values are plotted and are found
 330 in good agreement: values from flow experiments on the decreasing step and values from the
 331 stationary state from creep step (see later in **Figures 16-18**). In the presence of 0.01M NaCl, the
 332 orientation stress increases up to almost 15 Pa. A higher energy is required to align the system due
 333 to partial screening of the electrostatic interactions (**Figure 14**). This is in agreement with the lower
 334 order parameter as shown in X-rays and the appearance of a plateau in the $\sigma(\dot{\gamma})$ representation
 335 (**Figure 15**). In the presence of 0.1M NaCl, a smooth variation of the viscosity as a function of stress
 336 is obtained and is in good agreement with absence of a plateau in $\sigma(\dot{\gamma})$ representation (**Figure 15**).



337
338
339
340

Figure 14. Viscosity as a function of the shear stress at 25°C in H₂O, 0.01M NaCl and 0.1M NaCl. Measures were performed on decreasing shear rate sweep (open symbols) and in the stationary state from creep step (filled symbols).



341
342
343

Figure 15. Shear stress as a function of the shear rate for DNA 10 mg/mL solution at 25°C in H₂O, 0.01M NaCl and 0.1M NaCl.

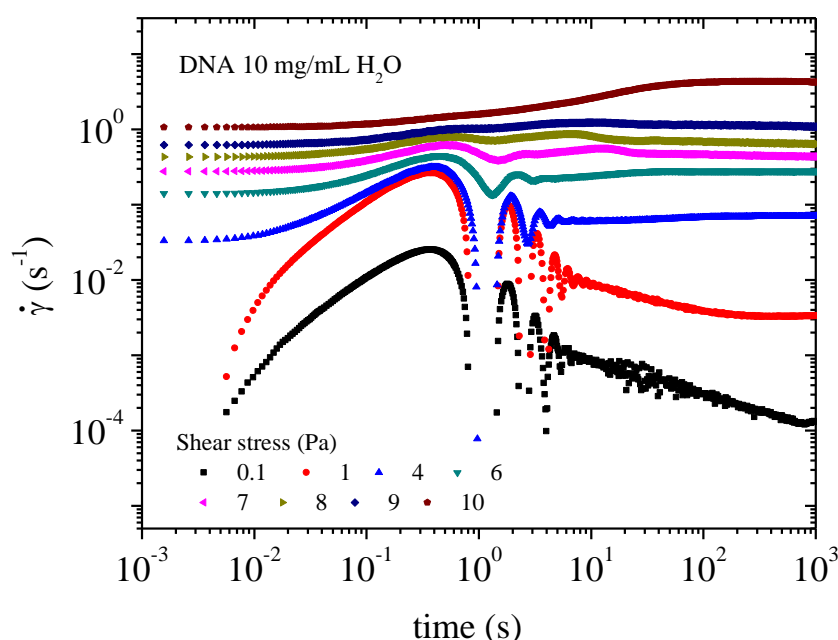
344
345
346

In the representation $\sigma(\dot{\gamma})$, the presence of a plateau corresponds to the appearance of textures as shown in **Figure 5a** and **b**. In the same conditions as in rheological experiments, in water, texture occurs directly over 1 s^{-1} (i.e., 5 Pa, **Figure 5a**) and continues forming at a nearly constant shear stress

347 (10 Pa) at which the viscosity drops (Figure 14) giving a plateau in the $\sigma(\dot{\gamma})$ curve (Figure 15). In 0.01M
 348 NaCl DNA solution a transition occurs around 5 Pa. This corresponds to the appearance of an
 349 equivalent texture (Figure 5 b). The transition is completed at a constant shear stress (12 Pa) before
 350 the viscosity drops. This drop in viscosity corresponds to a plateau in the $\sigma(\dot{\gamma})$ curve. The vertical
 351 viscosity drop is longer in water than in 0.01M NaCl. This is due to the decrease of electrostatic
 352 interchain interactions in the presence of external salt. In 0.1MNaCl DNA solution, the viscosity
 353 decreases progressively as a function of stress applied (Figure 14). Unlike in water and 0.01M NaCl
 354 solutions, no texture is observed (Figure 5c). Above shear stress of 8 Pa, an heterogenous birefringent
 355 solution organization across the entire volume is obtained indicating the orientation of large
 356 associated domains going to fully birefringent solution at high shear stress. Irrespective of the
 357 solvent, for shear stresses greater than 15-20 Pa, complete orientation of DNA forms a pseudo-
 358 nematic phase as suggested (birefringence is maximum) [11].

359 3.3.3. Transient regime

360 The transitory state is defined when constant shear stress is applied. Creep experiments enable
 361 this regime to be studied. In water, at 10^{-2} Pa, no flow occurs (Figure 16). After transient inertia
 362 viscoelastic coupling, the shear rate decreases until 10^{-4}s^{-1} for 10^3s , indicating a solid like behavior in
 363 water (as indicated in Figure 10). The sample starts flowing at 10^{-1} Pa corresponding to $3 \times 10^{-3}\text{s}^{-1}$.
 364 Flow is accompanied by a change in the polymer structure when the network is ruptured as
 365 evidenced by a rapid decrease in viscosity (Figure 12). The first oscillations in Figure 16 occur at a
 366 characteristic time, which is progressively shifted for stress applied higher than 5 Pa. At 7 Pa the
 367 oscillations disappear giving a bump around 10 s corresponding to the transition in shear stress
 368 (Figure 14). Over 9 Pa, corresponding to the pseudo plateau in shear stress versus shear rate
 369 representation, when the texture is observed the supramolecular structure is stabilized very rapidly.

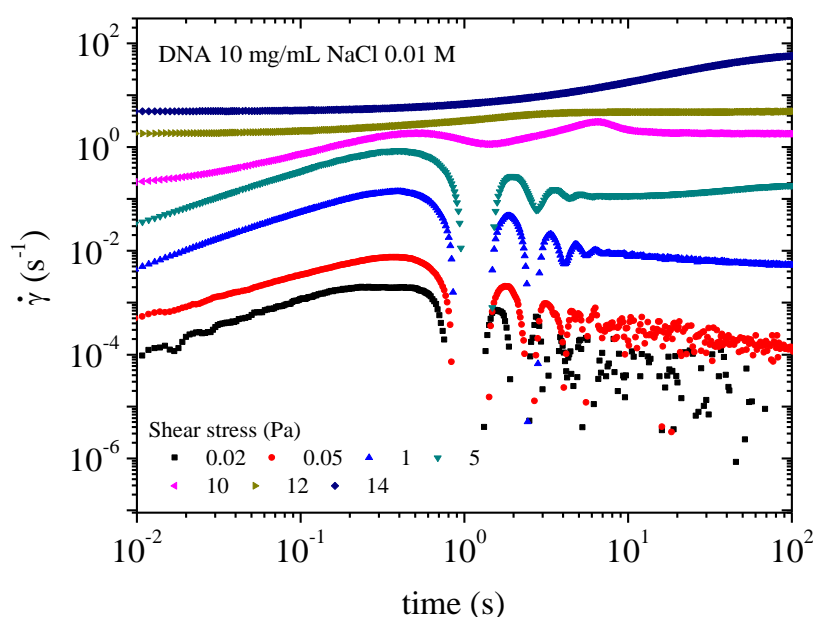


370

371 **Figure 16.** Transient behavior for DNA solution 10mg/mL in water: creep experiment giving the shear
 372 rate as a function of time for each stress applied from 0.1 to 10 Pa.

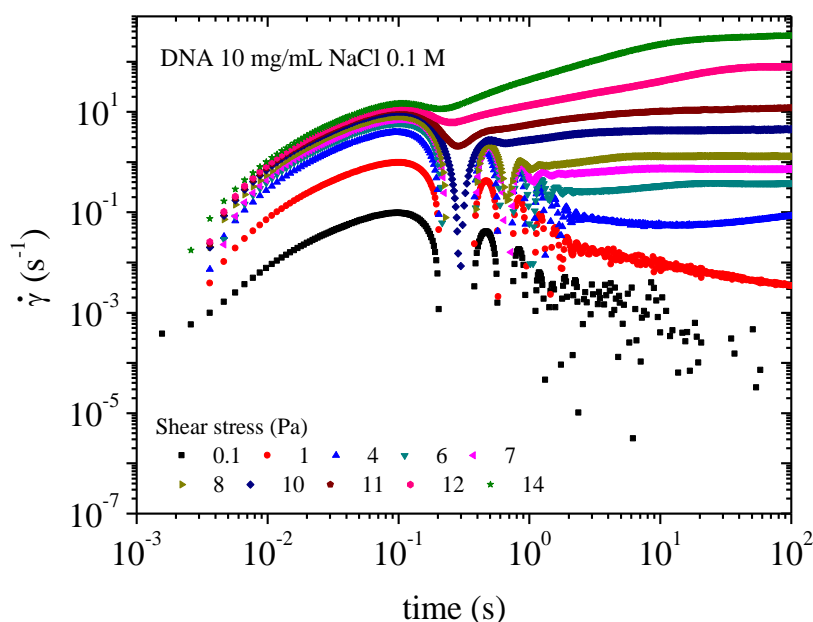
373 A similar behavior is observed in the presence of 0.01 M NaCl. At very low stress (circa 0.02 Pa)
 374 the sample behaves as a solid (Figure 17). The sample begins to flow at a lower yield stress than the
 375 sample in water and is faster to reach the stationary state. For samples in 0.01 M NaCl solution flow
 376 occurs at circa 1 Pa, and the stationary state is obtained after a maximum of 100 s. When stress above

377 10 Pa is applied the sample exhibits a textured structure under birefringence. Physically this behavior
 378 is caused by a looser electrostatic network providing less hindrance to movement than for DNA in
 379 water solution corresponding to lower viscosity (Figure 12).



380

381 **Figure 17.** Transient behavior for DNA solution 10mg/mL in water: creep experiment giving the shear
 382 rate as a function of time for each stress applied from 0.1 to 10 Pa.



383

384 **Figure 18.** Transient behavior for DNA solution 10mg/mL) in 0.1M NaCl: creep experiment giving the
 385 shear rate as a function of time for each stress applied from 0.1 to 14 Pa.

386 In 0.1M NaCl, the flow occurs at very low shear stress corresponding to an apparent yield stress
 387 lower than 0.1 Pa (Figure 18). In this salt concentration, the supramolecular organization changes to
 388 a looser structure.

389 Irrespective of solvent conditions, the DNA solutions at 10 mg/mL present a yield stress at very
390 low shear stress in agreement with dynamical and flow measurements (**Figures 10 and 12**).

391 4. Conclusions

392 The influence of the external salt concentration on the rheology and supramolecular structure of
393 DNA solutions was discussed in this paper. Rheological measurements were performed with SAXS
394 and birefringence experiments. In water, strong interchain electrostatic repulsions induced the
395 existence of a correlation peak between chains in solution. This correlation peak is progressively
396 depressed in presence of external salt. Two DNA concentrations in the semi entangled regime were
397 chosen: 4mg/mL which exhibits birefringence at high shear rates, but no particular texture is
398 observed; and 10 mg/mL where clear supramolecular structure was evidenced previously in 0.01M
399 buffer solution [11].

400 At 4 mg/mL in water, the G' modulus and the viscosity under flow are higher than in presence
401 of salt. Viscosity decreases steeply around a stress of 5 Pa and birefringence occurs over 50 s^{-1}
402 corresponding to alignment of all the chains in the flow. Salt in solution changes the rheological
403 behavior due to screening of electrostatic repulsions. The local organization is depressed but it is
404 shown that the dynamic modulus and flow viscosity are lower in 0.01M NaCl than in 0.1M NaCl. In
405 this case, 0.1 M NaCl concentration, long range electrostatic interactions are absent and steric
406 interactions dominate in the entangled semi-rigid chain assembly, inducing higher G' and viscosity
407 in the Newtonian plateau.

408 Irrespective of ionic concentration, increasing the stress progressively allows orienting the
409 interacting chains and the curves obtained for the different solvents superimpose over a stress around
410 2 Pa (**Figure 9**). Larger stresses correspond to the entrance in the birefringent regime where all the
411 chains orient in the flow over 4 Pa. Clearly, from **Figure 9**, a smooth transition is obtained confirming
412 the absence of plateau on $\sigma(\dot{\gamma})$ representation.

413 At 10 mg/mL, an electrostatic network with $G'(\omega) = G''(\omega)$ is demonstrated from dynamic
414 rheology at frequency lower than 0.08 rad/s in water; electrostatic interactions decrease progressively
415 in presence of external salt being progressively substituted by steric interactions. Then, an apparent
416 yield stress is found from stress measurement at low shear rate and confirmed in transient
417 experiments in water and to a lower degree in NaCl. Due to this mechanism, viscosity measurements
418 as a function of the shear rate are delicate and the values must be taken on the decreasing step in
419 shear rate. Due to this gelation mechanism, observation time dependence involved in experiments
420 under stress implies change in the supramolecular structure and dynamic of the systems.

421 The curves giving the viscosity as a function of the shear stress applied presents a two steps
422 transition: i) first one around 4 Pa (over 1 s^{-1}) where texture starts; the second one at 10 Pa in water;
423 ii) at 4 Pa and around 12 Pa in 0.01M NaCl respectively corresponding to texture appearance with
424 large decrease in viscosity at constant shear stress. The formation of the texture corresponds to a
425 plateau in the shear stress (shear rate) representation. Textures in 0.01M NaCl are less visible than
426 in water corresponding to a lower organization of stiff chains. Nevertheless, in 0.1M NaCl, smooth
427 variation of the viscosity with shear stress with looser organization (no texture as shown in water
428 and 0.01M NaCl) is obtained with no plateau in the stress versus shear rate representation. In 0.1M
429 NaCl, heterogeneous birefringent solution formed by large domains orientated in the flow. Whatever
430 the ionic conditions, at higher shear stress, all the chains orient in the flow with a low viscosity and
431 the solutions are birefringent corresponding a pseudo-nematic supramolecular organization of the
432 system.

433 This work clearly describes the influence of polymer concentration and external ionic
434 concentration on the rheological behavior and supramolecular structure of this original stiff DNA
435 polymer. It is demonstrated that at higher polymer concentration, a plateau is obtained in the $\sigma(\dot{\gamma})$
436 representation as soon as long-range electrostatic interactions and texture exist. An important point
437 is that the rheology is dependent on the history of the samples at higher polymer concentration (as
438 seen in the example of DNA solution at 10mg/mL). The experimental conditions need to be precisely
439 controlled, especially the ramp speed in viscosity and shear rate experiments, to obtain robust data.

440 For the first time, the presence of an electrostatic network is demonstrated, especially in water
441 at 10 mg/mL DNA concentration where electrostatic repulsions are at a maximum. In addition, for
442 all samples studied it is shown that the rheological behavior is particularly original at low flow shear
443 rate and low dynamic frequency applied.

444 **Supplementary Materials:** The following are available online at www.mdpi.com/link, Video S1, S2: DNA
445 solutions 10 mg/mL in water and in 0.1M NaCl under shear are joined in SI.

446 **Acknowledgments:** We acknowledge the European Synchrotron Radiation Facility for providing synchrotron
447 radiation facilities and we would like to thank Theyencheri Narayanan and Sylvain Prévost for assistance in
448 using beamline ID02. L.M. Bravo-Anaya acknowledges the fellowship grant given by CONACYT (CVU 350759).
449 Laboratoire Rhéologie et Procédés is a part of the LabEx Tec21 (Investissements d’Avenir–Grant agreement no.
450 ANR-11-LABX-0030), of PolyNat Carnot Institut (Investissements d’Avenir–Grant agreement no. ANR-11-
451 CARN-030-01) and of the program ANR-15-IDEX-02. We acknowledge M. Karrouch and E. Faivre from
452 Laboratoire Rhéologie et Procédés, Grenoble, for their valuable help and technical support.

453 **Author Contributions:** Lourdes Mónica Bravo Anaya and Marguerite Rinaudo suggested the work; Lourdes
454 Mónica Bravo-Anaya, Marguerite Rinaudo, Denis Roux and Frédéric Pignon conceived and designed the
455 experiments; Lourdes Mónica Bravo-Anaya, J.F. Armando Soltero Martínez, Francisco Carvajal Ramos and
456 Oonagh Manix performed the experiments; Marguerite Rinaudo, Denis Roux, Oonagh Manix, Lourdes Mónica
457 Bravo-Anaya and Frédéric Pignon analyzed the data; J.F. Armando Soltero Martínez and Francisco Carvajal
458 Ramos contributed with reagents; Marguerite Rinaudo and Denis Roux wrote the paper.

459 **Conflicts of Interest:** the authors declare no conflict of interest.

460 Abbreviations

461 DNA: Deoxyribonucleic Acid

462 SAXS: Small-angle X-ray scattering

463 References

- 464 1. Maret, G.; Weill, G. Magnetic birefringence study of the electrostatic and intrinsic persistence length of
465 DNA, *Biopolymers*, **1983**, *22*, 2727–2744.
- 466 2. Odijk, T. On the Ionic-Strength Dependence of the Intrinsic Viscosity of DNA *Biopolymers*, **1979**, *18*, 3111-
467 3113.
- 468 3. Manning, G.S. The Persistence Length of DNA Is Reached from the Persistence Length of Its Null Isomer
469 through an Internal Electrostatic Stretching Force, *Biophys. J.*, **2006**, *91*, 3607–3616.
- 470 4. Odijk, T. Possible scaling relations for semidilute polyelectrolyte Solutions. *Macromolecules*, **1979**, *12*,
471 688–693.
- 472 5. Malovikova, A.; Milas, M.; Rinaudo, M.; Borsali, R. Viscosimetric behavior of Na-polygalacturonate in the
473 presence of low salt content, *Macro-ion characterization from dilute solutions to complex fluids*, ACS Symp.
474 Series 548, K.S. Schmitz Ed., ISBN 0841227705, **1994**, 315–321.
- 475 6. Ray, J. ; Manning, G. S. Formation of Loose Clusters in Polyelectrolyte Solutions, *Macromolecules* **2000**, *33*,
476 2901–2908.
- 477 7. Ray, J. ; Manning, G. S. An Attractive Force between Two Rodlike Polyions Mediated by the Sharing of
478 Condensed Counterions, *Langmuir* **1994**, *10*, 2450–2461.
- 479 8. Manning, G.S. Counterion condensation theory of attraction between like charges in the absence of
480 multivalent counterions, *Eur. Phys. J. E* **2011**, *34*, 132–149.
- 481 9. Wissenburg, P.; Odijk, T.; Cirkel, P.; Mandel, M. Multimolecular Aggregation in Concentrated Isotropic
482 Solutions of Mononucleosomal DNA in 1 M Sodium Chloride, *Macromolecules*, **1994**, *27*, 306–308.
- 483 10. Wissenburg, P.; Odijk, T.; Cirkel, P.; Mandel, M. Multimolecular Aggregation of Mononucleosomal DNA
484 in Concentrated Isotropic Solutions, *Macromolecules*, **1995**, *28*, 2315–2328.
- 485 11. Bravo-Anaya, L. M.; Macias, E.R.; Pérez-López, J.H.; Galliard, H.; Roux, D.; Landazuri, G.; Carvajal Ramos,
486 F.; Rinaudo, M.; Pignon, F.; Soltero, J.F.A. Supramolecular organization in calf-thymus DNA solutions
487 under flow in dependence with DNA concentration. *Macromolecules*, **2017**, *50* (20), 8245–8257.
- 488 12. Nierlich, M.; Williams, C.E.; Boue, F.; Cotton, J.P.; Daoud, M.; Farnoux, B.; Jannink, G.; Picot, C.; Moan, M.;
489 Wolff, C.; Rinaudo, M.; De Gennes, P.G. Small angle neutron scattering by semi-dilute solutions of
490 polyelectrolyte, *J. Phys.*, **1979**, *40*, 701–704.

- 491 13. Morfin, I.; Reed, W.F.; Rinaudo, M.; Borsali, R. Further evidence of liquid-like correlations in polyelectrolyte
492 solutions, *J. Phys. II*, **1994**, *4*(6), 1001-1019.
- 493 14. Borsali, R. ; Rinaudo, M. ; Noirez, L. Light scattering and small-angle neutron scattering from
494 polyelectrolyte solutions: the succinoglycan. *Macromolecules*, **1995**, *28*(4), 1085-1088.
- 495 15. Milas, M. ; Lindner, P. ; Rinaudo, M. ; Borsali, R. Influence of the shear rate on the small-angle neutron
496 scattering pattern of polyelectrolyte solutions: the xanthan example. *Macromolecules*, **1996**, *29*(1), 473-474.
- 497 16. Pringle, O. A. ; Schmidt, P. W. Small-angle X-ray scattering from helical macromolecules. *J. Appl.*
498 *Crystallogr.*, **1971**, *4*(4), 290-293.
- 499 17. Potemkin, I. I. ; Vasilevskaya, V. V. ; Khokhlov, A. R. Associating polyelectrolytes: finite size cluster
500 stabilization versus physical gel formation. *J. Chem. Phys.*, **1999**, *111*(6), 2809-2817.
- 501 18. Moan, M. ; Wolff, C. Study of the conformational rigidity of polyelectrolytes by elastic neutron scattering:
502 1. Carboxymethylcelluloses in the intermediate momentum range. *Polymer*, **1975**, *16*(11), 776-780.
- 503 19. Larson R.G. Liquid-crystalline Polymers, in *The structure and rheology of complex fluids*, Chap. 11, Oxford
504 University Press, New-York, **1999**, 503-550.
- 505 20. Yamanaka, J. ; Matsuoka, H. ; Kitano, H. ; Hasegawa, M., ; Ise, N. Revisit to the intrinsic viscosity-molecular
506 weight relationship of ionic polymers. 2. Viscosity behavior of salt-free aqueous solutions of sodium poly
507 (styrenesulfonates). *J. Am. Chem. Soc.*, **1990**, *112* (2), 587-592.
- 508 21. Winter, H. H. ;Chambon, F. Analysis of linear viscoelasticity of a crosslinking polymer at the gel point. *J.*
509 *Rheol.*, **1986**, *30*(2), 367-382.
- 510 22. Winter, H.H. ; Mours M. Rheology of polymers near liquid-solid transitions, in *Advances in Polymer Science*,
511 *14*, Springer-Verlag Berlin (Germany) **1997**, 165-234.
- 512 23. Winter, H.H. Glass transition as the Rheological Inverse of Gelation, *Macromolecules* **2013**, *46*, 2425-2432.
- 513 24. Barnes, H. A. A review of the slip (wall depletion) of polymer solutions, emulsions and particle
514 suspensions in viscometers: its cause, character, and cure. *J Nonnewton Fluid Mech.*, **1995**, *56*(3), 221-251.
- 515 25. Barnes, H. A. The yield stress—a review or ‘ $\pi\alpha\nu\tau\alpha\ \rho\epsilon\iota'$ —everything flows?. *J Nonnewton Fluid Mech.* **1999**,
516 *81*(1-2), 133-178.
- 517 26. Auffret, Y. ; Roux, D. C. D. ; El Kissi, N. ; Dunstan, D. E. ; Pignot-Paintrand, I. Stress and strain controlled
518 rheometry on a concentrated lyotropic lamellar phase of AOT/Water/Iso-octane. *Rheol. Acta*, **2009**, *48*(4),
519 423-432.
- 520 27. Saramito, P. A new constitutive equation for elastoviscoplastic fluid flows. *J Nonnewton Fluid Mech.*, **2007**,
521 *145*(1), 1-14.
- 522 28. Cheddadi, I. ; Saramito, P. ; Graner, F. Steady Couette flows of elastoviscoplastic fluids are nonunique. *J.*
523 *Rheol.*, **2012**, *56*(1), 213-239.
- 524 29. Meeker, S. P. ; Bonnecaze, R. T. ; Cloitre, M. Slip and flow in pastes of soft particles: direct observation and
525 rheology. *J. Rheol.*, **2004**, *48*(6), 1295-1320.



© 2018 by the authors. Submitted for possible open access publication under the terms and conditions of the Creative Commons Attribution (CC BY) license

528 (<http://creativecommons.org/licenses/by/4.0/>).